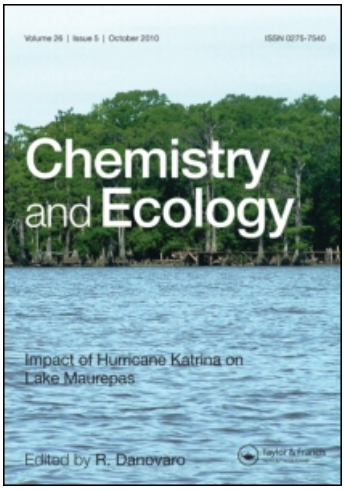

Chemistry and Ecology
Publication details, including instructions for authors and subscription information:
http://www.informaworld.com/smpp/title~content=t713455114

Impact of calcium and magnesium on growth and morphological acclimations of *Nitella*: implications for calcification and nutrient dynamics

Pattiyage I. A. Gomes[a]; Takashi Asaeda[b]
[a] Department of Civil and Environmental Engineering, University of Ruhuna, Galle, Sri Lanka [b] Institute for Environmental Science and Technology, Saitama University, Saitama, Japan

Online publication date: 04 December 2010

To cite this Article Gomes, Pattiyage I. A. and Asaeda, Takashi(2010) 'Impact of calcium and magnesium on growth and morphological acclimations of *Nitella*: implications for calcification and nutrient dynamics', Chemistry and Ecology, 26: 6, 479 — 491
To link to this Article: DOI: 10.1080/02757540.2010.504667
URL: http://dx.doi.org/10.1080/02757540.2010.504667

Chemistry and Ecology
Vol. 26, No. 6, December 2010, 479–491

Taylor & Francis
Taylor & Francis Group

Impact of calcium and magnesium on growth and morphological acclimations of *Nitella*: implications for calcification and nutrient dynamics

Pattiyage I.A. Gomes[a]* and Takashi Asaeda[b]

[a] *Department of Civil and Environmental Engineering, University of Ruhuna, Galle, Sri Lanka;* [b] *Institute for Environmental Science and Technology, Saitama University, Saitama, Japan*

(*Received 22 December 2009; final version received 8 June 2010*)

The impact of calcium (Ca) and magnesium (Mg) on the growth and morphology of a Charophyte, *Nitella pseudoflabellata*, and the influence of Mg on calcification and phosphorous (P) speciation were studied in laboratory experiments for variable concentrations ($\leqq 120\,\mathrm{mg \cdot L^{-1}}$) of Ca and Mg. It was clearly identified that Mg aided shoot elongation. An increase in Ca concentrations produced intensified shoot elongation also, but at a lesser rate than the equivalent levels of Mg. Depending on the availability of Ca and Mg, the morphological appearance differed significantly, suggesting significant levels of ecoplasticity. Furthermore, Mg was observed to produce less calcite encrustation. Plant P-speciation suggested a higher Mg concentration corresponding to a more water-soluble and less carbonate-bound P fraction. This indicates that upon senescence and decomposition, a large fraction of P is supplied to the water column; ultimately behaving similar to a typical vascular plant.

Keywords: calcium; calcification; magnesium; *Nitella pseudoflabellata*; phosphorous

1. Introduction

Charophytes, the growth form of characean algae, occur in a wide range of water bodies [1]. They grow completely submerged in the water of wetlands, rivers, streams, lakes, estuaries and swamps: in fact, in all kinds of non-marine watery habitats [1,2]. It is often argued that the presence of charophytes indicates a healthy clear water ecosystem [1,3,4], however, some authors have reported them to be a nuisance plant [5]. Charophytes are often pioneer plants in newly created or inundated wetlands [6], and also in artificial wetlands [3]. Furthermore, reports suggest that they are pioneers for colonisation in water bodies following a disturbing event [7]. Charophytes can easily adapt their life-cycle to water-level fluctuations and they provide habitat and food for macroinvertebrates [3]. Thus, they are considered an ideal plant for the development of functional wetlands. Recent research also suggests that charophytes are potentially useful for the remediation of various pollutants (such as heavy metals) in natural and constructed wetlands [3,4].

*Corresponding author. Email: ishan_gomes@yahoo.com

ISSN 0275-7540 print/ISSN 1029-0370 online

DOI: 10.1080/02757540.2010.504667
http://www.informaworld.com

Charophytes are considered to be an algal class with extreme morphological complexity of thallus organisation and the gametangia structure [8]. Furthermore, they exhibit a high degree of morphological variation, such that the size and length of organs differ depending on the conditions under which they grow [9–11]. This type of ecoplasticity [9] has contributed to difficulties in the taxonomy of these algae [12].

Many forms of charophyte are subject to calcification [13], which in the form of calcium carbonate ($CaCO_3$) takes place on stems, branchlets and on the surface of oogonia [9]. Calcification accompanies the photosynthetic utilisation of bicarbonate [14,15]. Most aquatic plants under hard water conditions are capable of precipitating calcite ($CaCO_3$) [16–18], however, the $CaCO_3$ is dispersed and is not associated with the plants themselves [17,19]. Charophytes are uncommon in the sense that calcite is not dispersed. Furthermore, charophytes have a higher calcifying potential than other aquatic plants [4]. Van den Berg et al. [20] reported charophytes containing $CaCO_3$ at levels as high as 60% per dry weight. It has also been reported that many heavily calcified charophytes are deposited in aquatic environments, leading to the formation of marl [13,19].

Aquatic macrophytes play an important role in nutrient cycling, due to the large quantities of biomass they produce and their capacity to accumulate large concentrations of nutrients [21–23]. In the context of charophytes, in particular, the absence of vascular tissue means that the above-ground parts play an important role in acquiring nutrients from the water column [24,25]. Otsuki and Wetzel [26] have stated that phosphorous (P) can become co-precipitated with photosynthetically induced calcite and stated it to be an important process in the reduction of nutrient bioavailability of P. Siong and Asaeda [17] have shown that calcification of the genus *Chara* has potential for a P nutrient sink.

Calcium (Ca) in water obviously plays a prominent role in the habitats of charophytes, in particular, the process of calcification and the Mg/Ca ratio influence the mineralogy of carbonate encrustations because the aragonite formations seem to be related to relatively high values of Mg/Ca, among other factors [27]. Many aquatic habitats often contain higher amounts of Ca than Mg. However, there are a number of charophyte habitats in which concentrations of Mg are far greater than the concentrations of Ca (e.g. $>100\,\mathrm{mg}\cdot\mathrm{L}^{-1}$ Mg, approximatley four times the Ca concentration, in Myall Lake, Australia) [28].

The objective of this research was to study the impact of Ca and Mg on the growth and morphology of a characean alga *Nitella pseudoflabellata*. The hypothesis that high Mg availability in water will result in the reduction of carbonate-bound P was also tested. Through this, it was possible to evaluate the likelihood of P nutrient cycling in aquatic habitats dominated by charophyte beds.

2. Materials and methods

2.1. *General culture methods and materials*

Collections of *N. pseudoflabellata* were originally obtained from a pond near the Teganuma Lake (35.5° N 140.0° E) Chiba, Japan. The collected specimen was placed in an aquarium and plants seen to be growing well were harvested and planted in a 50-L tank containing 20 kg of commercially available river sand (90% <1 mm; DIY, Doite®, Japan) and distilled water (sand was added and water was topped up to the 50 L level). Sand used for culturing was washed extensively with tap water to remove dust particles, until the supernatant was found to be clear. Finally, it was rinsed with distilled water. After drying, sand was sealed in gallon jars and stored until use. In this washed sand and distilled water *N. pseudoflabellata* showed satisfactory growth without the appearance of contaminating algae such as *Oscillatoria* spp., and all experiments utilised this basic combination of sand and water. The plants were allowed to grow axenically in the 50-L tank for approximately one year at a controlled temperature of 24–25 °C.

Table 1. Ca and Mg concentrations of Ca-treated, Mg-treated, and Ca- and Mg-treated units. Concentrations are given in $mg \cdot L^{-1}$.

Ca-treated		Mg-treated		Ca- and Mg-treated	
Ca	Mg	Ca	Mg	Ca	Mg
4	2	4	4	40	40
40	2	4	40	40	120
80	2	4	80	80	80
120	2	4	120	120	40

2.2. *Experiment 1*

A laboratory experiment was carried out using 1-L beakers (Iwaki Pyrex®, Japan) for a period of nine weeks for different concentrations of Ca (4, 40, 80 and 120 $mg \cdot L^{-1}$), Mg (4, 40, 80 and 120 $mg \cdot L^{-1}$) and combinations of Ca and Mg (40, 40; 40, 120; 80, 80; and 120, 40 $mg \cdot L^{-1}$ of Ca and Mg, respectively); these treatments are referred to as 'Ca-treated', 'Mg-treated' and 'Ca- and Mg-treated' (Table 1). Each treatment was duplicated and the entire experiment was repeated. Maximum concentrations of Ca and Mg were decided upon by referring to concentrations reported in natural habitats of charophytes [9,28]. The experimental beakers consisted of 400 g of washed river sand with distilled water, filled to 1 L. The desired concentrations of Ca and Mg were achieved by adding $CaCl_2 \cdot 2H_2O$ (analytical reagent grade; Sigma-Aldrich®) and $MgCl_2 \cdot 6H_2O$ (analytical reagent grade; Sigma-Aldrich®), respectively. Owing to mixing with the substrate, the minimum levels that could be maintained for Ca and Mg were 4 and 2 $mg \cdot L^{-1}$, respectively. Total phosphorous was observed to be $\sim 75\ \mu g\ L^{-1}$. The pH of the medium was slightly alkaline, ~7.5, without significant difference between treatments. All units were kept in a water bath at a constant temperature of 24 °C. Three heaters (IC AUTO NEO type 180, NISSO, Japan) were used to maintain the desired temperature, and the water was mixed mechanically to provide a homogeneous temperature. Illumination was supplied using 4 × 20 W fluorescent lamps (Kyushu Denki Hanabai Corporation, Japan) with a photoperiod of 12 h light and 12 h dark.

Apical tips of uncalcified *N. pseudoflabellata* (2–3 internodes, 2–3 cm length) with similar morphological features were harvested from the 50 L tank and planted in 1 L beakers, for each 10 tips, positioning 2–2.5 internodes (~2 cm) above the substrate. Three were used for growth measurements (shoot elongation) and the remainder were used for the end experiment analysis of plant Ca and Mg levels. Apical tips used for elongation measurements had virtually the same above-ground shoot length and morphology. Each week, shoot length was recorded. Shoot elongation was calculated as the percentage of shoot length increase relative to the initial shoot length [4]:

$$E = (L_t - L_o) \times 100/L_o,$$

where E is the shoot elongation (% relative to the initial length) at week t, L_t is the cumulative average shoot length in the tth week and L_o is the average initial shoot length. Shoot elongations were recorded up until the ninth week.

We used a linear model to represent shoot elongation against time [4,13,28,29]. Thus the gradient of the line of best fit between shoot elongation and time was used to identify the elongation per week (e). Sampling for plant Ca and Mg was carried out during the ninth week.

2.3. *Experiment 2*

Another experiment was carried out for a period of six months, for four combinations of water having variable concentrations of Ca and Mg (40, 40; 40, 120; 80, 80; and 120, 40 $mg \cdot L^{-1}$ for Ca and

Mg, respectively; the concentrations were the same as the Ca- and Mg-treated units of experiment 1; see Table 1) in 5 L tanks with similar conditions as in experiment 1 and each treatment was duplicated. Plant sampling was carried out at the end of the sixth month for P speciation.

2.4. *Chemical and physical analyses*

The temperature and pH of the beaker water were monitored continuously using a pH/temperature electrode (HM-25R Benchtop series, TOA-DKK, Japan). The same electrode was used to continuously monitor the temperature of the water bath. Harvested plants were oven dried (65 °C for 24 h), then weighed and ashed for 1 h at 550 °C, and dissolved in 1.0 M HNO_3 solution (double-distilled purified, Sigma–Aldrich®). After this, they were heated on a hotplate (Yamato HK 200, Japan) at 80 °C for 3 h [30]. Plant Ca and Mg levels (wavelengths of 422.7 and 285.2 nm, respectively) were analysed using an atomic absorption spectrophotometer (AA-6300 Shimadzu, Japan). The total phosphorous of water were measured using an auto-analyser (TRAACS 800, Technicon®, New York, USA). The Ca and Mg concentrations of the water were analysed using the EDTA titration method [30].

Plant P-speciation was carried out according to Siong and Asaeda [17] to determine P-speciation as water-soluble P (H_2O-P), nonreactive organic P (NaOH-P) and carbonate-bound P (HCl-P). The procedure was carried out for a plant sample size of 50–75 mg: 1) H_2O-P was extracted with 50 mL of distilled water for 30 min; (2) NaOH-P was extracted using 50 mL of 1.0 M NaOH for 20 h; and (3) HCl-P was extracted using 1.0 M HCl for 30 min. The phosphorous concentration in the extract was determined using the molybdenum blue colorimetric method [31]. Acid or alkaline extract was neutralised prior to this. Phosphorous in NaOH extract was measured following digestion with $K_2S_2O_8$ in an autoclave (120 °C) for 30 min [30]. Further Ca and Mg in HCl-P were also measured using atomic absorption spectrophotometer.

At the end of ninth week, plants used for elongation measurements (experiment 1) were investigated under a microscope (Olympus BX40, Japan) to determine branchlet lengths. Two whorls of the middle (or near middle) internode were used for this purpose. The total number of sexual propagules (oogonium and antheridium) was counted in these plants.

For chlorophyll fluorescence analysis, plants were immersed in a solution taken from their relevant beakers and kept in the dark for 15 min. Chlorophyll fluorescent analysis (Photon Systems Instruments Handy FC 1000-H, Czech Republic) was conducted with auto-image segmentation. Maximum quantum efficiency of PSII photochemistry (F_v/F_m) was used as the stress indicator for plants.

2.5. *Statistical analysis*

All data are presented mean ± SD. Assumption of normal distribution and the homogeneity of variances were checked using Kolmogorov–Smirnov and Levene's tests, respectively, on data sets prior to statistical analyses. One-way analysis of variance (ANOVA) with a Tukey's post-hoc test was used to compare means. All p-values were considered significant at <0.05. Correlation between two variables was checked using Pearson's correlation (r) analysis with a two-tailed significance test ($p < 0.05$). For this purpose, SPSS for Windows (release 13, SPSS Inc., Chicago, IL, USA) statistical software package was used.

CANOCO 4.5® was used for relationship building among response variables and explanatory variables. Redundancy analysis (RDA) was selected based on the short gradient length of <4 [32]. Conditional effects of explanatory data on response data was assessed using the Monte Carlo permutation test, under full model with automatic variable selection using Canoco for Windows [32].

3. Results

3.1. *Shoot elongation at variable concentrations of Ca, Mg and bivariant concentrations of Ca and Mg*

Figure 1(a)–(c) illustrates temporal variation in shoot elongation for different Ca-treated, Mg-treated and Ca- and Mg-treated units respectively. Figure 1(a) shows that an increase in Ca concentrations led to an increase in the temporal variation in elongation. Furthermore, the elongation achieved at the end of ninth week by plants in the unit with $120\,\mathrm{mg}\cdot\mathrm{L}^{-1}$ Ca was observed to be significantly higher (ANOVA, $p < 0.05$) than plants grown in units with 4 and $40\,\mathrm{mg}\cdot\mathrm{L}^{-1}$ Ca. The Ca concentrations and elongation at the end of the ninth week showed a strong positive correlation ($r = 0.91$, $p < 0.01$). According to Figure 1(b), with increasing Mg concentrations, the temporal variation in elongation also increased. However, the difference in elongation observed at the end of ninth week was found to be insignificant (ANOVA, $p > 0.05$) between all Mg-treated units, except for the unit with $4\,\mathrm{mg}\cdot\mathrm{L}^{-1}$ Mg. This unit showed significantly less (ANOVA, $p < 0.05$) elongation at the end of ninth week compared with the remaining Mg-treated units. The Mg concentrations and elongation at the end of ninth week also showed a positive correlation ($r = 0.88$, $p < 0.01$). Considering the temporal variation in the elongation of Ca- and Mg-treated units (Figure 1(c)), the highest elongation measured at ninth week was achieved in the unit with $40\,\mathrm{mg}\cdot\mathrm{L}^{-1}$ Ca and $120\,\mathrm{mg}\cdot\mathrm{L}^{-1}$ Mg. This was closely followed by $80\,\mathrm{mg}\cdot\mathrm{L}^{-1}$ Ca and $80\,\mathrm{mg}\cdot\mathrm{L}^{-1}$ Mg. The lowest elongation at the end of ninth week was observed in the unit with $120\,\mathrm{mg}\cdot\mathrm{L}^{-1}$ Ca and $40\,\mathrm{mg}\cdot\mathrm{L}^{-1}$ Mg. These observations suggest that Mg is increasing shoot elongation.

3.2. *Morphology and reproductive acclimations*

The internodal length in shoots measured at the end of the ninth week for Ca-treated units was seen to shorten with increased Ca concentrations ($r = -0.99$, $p < 0.01$). Furthermore, Mg-treated units ($\geq 40\,\mathrm{mg}\cdot\mathrm{L}^{-1}$ Mg) showed significantly greater (ANOVA, $p < 0.05$) internodal length for shoots relative to Ca-treated units. Primary and secondary branchlet lengths (Table 2) in Mg-treated units were also larger relative to Ca-treated units. With respect to tertiary branchlets (Table 2), Mg-treated units ($\geq 40\,\mathrm{mg}\cdot\mathrm{L}^{-1}$ Mg) showed significantly higher values in comparison with Ca-treated units (ANOVA, $p < 0.05$). Thus, these observations indicate that Mg is aiding growth.

Initially (in the fifth week), sexual propagules were observed in larger numbers in Ca-treated units than in Mg-treated units (data not shown). However, according to the count obtained at the end of ninth week (Table 2) no trend was identifiable with respect to type of treatment.

3.3. *Maximum quantum efficiency of PSII photochemistry (F_v/F_m)*

Table 2 illustrates the $F_\mathrm{v}/F_\mathrm{m}$ results obtained at the end of the ninth week for all treatments. In Ca-treated units, $F_\mathrm{v}/F_\mathrm{m}$ showed a negative correlation with Ca concentrations ($r = -0.97$, $p < 0.05$). Mg-treated units did not show any definite correlation with Mg concentration, however, the presence of Mg ($\geq 40\,\mathrm{mg}\cdot\mathrm{L}^{-1}$ Mg) gave an $F_\mathrm{v}/F_\mathrm{m}$ value >0.8. Plants from Mg-treated units ($\geq 40\,\mathrm{mg}\cdot\mathrm{L}^{-1}$ Mg) were seen to be more green than those from Ca-treated units ($\geq 40\,\mathrm{mg}\cdot\mathrm{L}^{-1}$ Ca), which were a slightly pale green in comparison. The lowest $F_\mathrm{v}/F_\mathrm{m}$ value of 0.76 ± 0.09 was seen in a plant from a Ca-treated unit ($120\,\mathrm{mg}\cdot\mathrm{L}^{-1}$ Ca).

3.4. *Ca and Mg accumulation by plants, and observations of calcification*

For many plants, no visual calcification was noticed (as per the ninth week). However, plants grown in 80 and $120\,\mathrm{mg}\cdot\mathrm{L}^{-1}$ Ca (Ca-treated units) showed symptoms of calcification. Microscopic

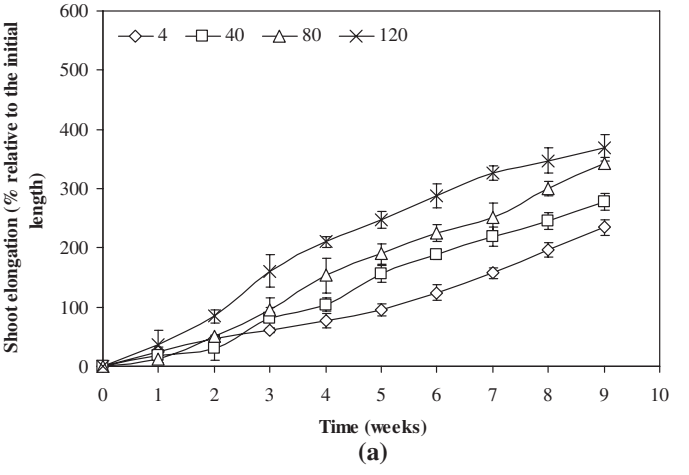

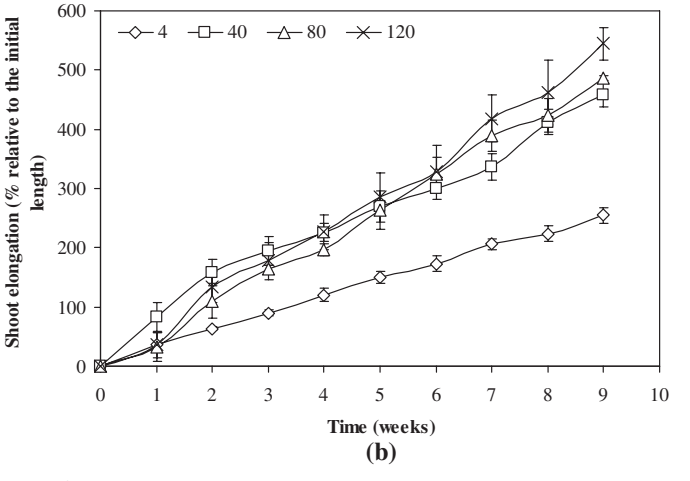

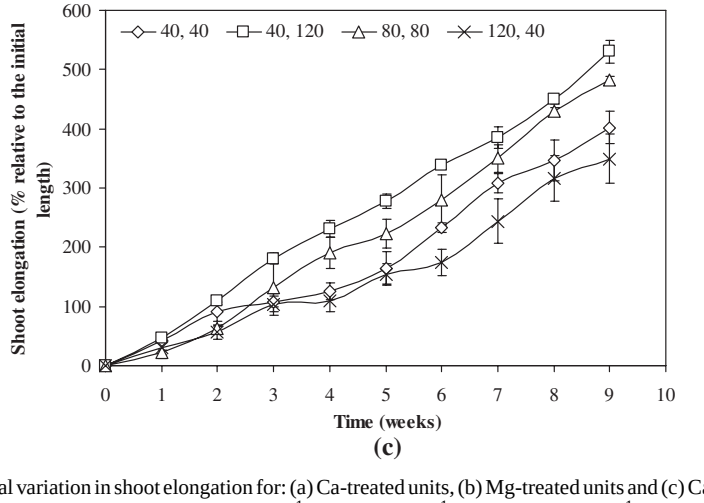

Figure 1. Temporal variation in shoot elongation for: (a) Ca-treated units, (b) Mg-treated units and (c) Ca- and Mg-treated units. Each legend indicates concentrations (a) $mg \cdot L^{-1}$ Ca, (b) $mg \cdot L^{-1}$ Mg, and (c) $mg \cdot L^{-1}$ Ca, $mg \cdot L^{-1}$ Mg.

Table 2. Explanatory and response variables of experiment 1.

CaW	MgW	e	CaP	MgP	IL	P	S	T	O	F_v/F_m
4	2	23.24	11.7 (0.6)	0.88 (0.06)	0.96 (0.05)	0.35 (0.01)	0.21 (0.02)	0.05 (0.04)	27	0.83 (0.05)
40	2	30.31	15.2 (1.1)	0.86 (0.01)	0.83 (0.21)	0.36 (0.01)	0.21 (0.01)	0.02 (0.02)	9	0.82 (0.06)
80	2	37.07	18.9 (0.9)	0.93 (0.01)	0.75 (0.01)	0.42 (0.09)	0.31 (0.03)	0.01 (0.00)	19	0.80 (0.07)
120	2	45.18	19.5 (0.3)	0.89 (0.04)	0.66 (0.18)	0.33 (0.03)	0.16 (0.03)	0.01 (0.00)	26	0.76 (0.09)
4	4	28.82	12.2 (0.3)	0.92 (0.05)	0.89 (0.05)	0.38 (0.03)	0.48 (0.07)	0.03 (0.04)	42	0.81 (0.04)
4	40	51.93	11.2 (1.2)	1.44 (0.06)	0.98 (0.02)	0.41 (0.01)	0.38 (0.04)	0.21 (0.03)	9	0.82 (0.04)
4	80	55.81	9.3 (0.7)	2.09 (0.21)	1.22 (0.12)	0.45 (0.01)	0.37 (0.03)	0.23 (0.03)	15	0.83 (0.05)
4	120	58.47	7.9 (0.8)	2.86 (0.11)	1.42 (0.10)	0.46 (0.02)	0.34 (0.03)	0.23 (0.07)	11	0.81 (0.05)
40	40	41.48	9.5 (0.5)	1.47 (0.04)	1.00 (0.05)	0.39 (0.01)	0.35 (0.04)	0.13 (0.06)	19	0.82 (0.05)
40	120	56.96	10.3 (1.5)	1.96 (0.21)	0.95 (0.06)	0.40 (0.01)	0.32 (0.02)	0.09 (0.01)	12	0.75 (0.07)
80	80	50.23	11.5 (1.7)	1.70 (0.07)	1.40 (0.34)	0.35 (0.03)	0.28 (0.02)	0.16 (0.03)	11	0.79 (0.05)
120	40	35.39	8.8 (0.5)	2.78 (0.18)	1.03 (0.06)	0.36 (0.01)	0.24 (0.03)	0.09 (0.01)	15	0.78 (0.07)

Notes: Explanatory variables: Ca and Mg concentrations of water in $mg \cdot L^{-1}$ (CaW, MgW). Response variables: Shoot elongation per week (e), Ca and Mg levels in plants in $mg \cdot g^{-1}$ (CaP, MgP). Internodal length (IL) in cm. Primary, secondary and tertiary branchlet lengths (P, S and T) in cm. Number of sexual propagules per plant (O) and maximum quantum efficiency of PSII photochemistry (F_v/F_m). Parentheses give SD values for means.

examinations revealed calcite encrustation in the form of regular bands on the stems and branchlets of all Ca-treated units. Of the Mg-treated units, only the $4\,mg \cdot L^{-1}$ Mg unit showed significant calcite encrustation. For combined treatments, the unit with $120\,mg \cdot L^{-1}$ Ca and $40\,mg \cdot L^{-1}$ Mg showed slight calcite encrustation on stems. Table 2 gives the Ca and Mg levels of plants (CaP and MgP) as measured at the end of the ninth week. Here, Ca-treated units showed a strong correlation between CaP and Ca concentrations ($r = 0.96$, $p < 0.05$). Interestingly, the CaP of Mg-treated units were seen to have a similar, but negative, correlation with Mg concentrations. This suggests that Mg is interacting with processes that absorb Ca into plants. However, no such interference was observed between Ca concentrations and Mg absorption by plants.

3.5. *Modelling of explanatory and response variables*

The biplot diagram for the redundancy analysis (RDA) based on all treatments (Ca-treated, Mg-treated and Ca- and Mg-treated) is shown in Figure 2. Table 2 shows all the values of response variables and explanatory variables. The explanatory variables used are the concentrations of Ca and Mg in water (CaW and MgW). The response variables include shoot elongation per week (e), Ca and Mg levels in plants (CaP and MgP), internodal length of shoots (IL), lengths of primary, secondary and tertiary branchlets (P, S and T), number of sexual propagules per plant (O) and maximum quantum efficiency of PSII photochemistry (F_v/F_m). Shoot elongation per week (e) showed positive correlation with MgW. Internodal length (IL), primary branchlet length (P) and tertiary branchlet length (T) also showed positive correlation with MgW, whereas they showed an almost similar negative correlation with CaW. Secondary branchlet length (S) showed a strong negative correlation with CaW, and a positive correlation with MgW. The number of sexual propagules per plant (O) did not show proper correlation with CaW, but did show a negative correlation with MgW. Furthermore, F_v/F_m did not show proper correlation with MgW, but a negative correlation with CaW. Mg levels measured in plants (MgP) showed a strong positive correlation with MgW, whereas they evidenced almost no correlation with CaW. However, CaP seemed to have equally positive and negative correlation with CaW and MgW, respectively. It should be noted that of the explanatory variables, only MgW was observed to be significant (Monte Carlo, $p < 0.05$; Table 3). Further, the highest ranking for conditional effects (Lamda-A) was proved to be MgW (Lamda-A explains the additional variance each variable explains at the time of inclusion to the model) [32].

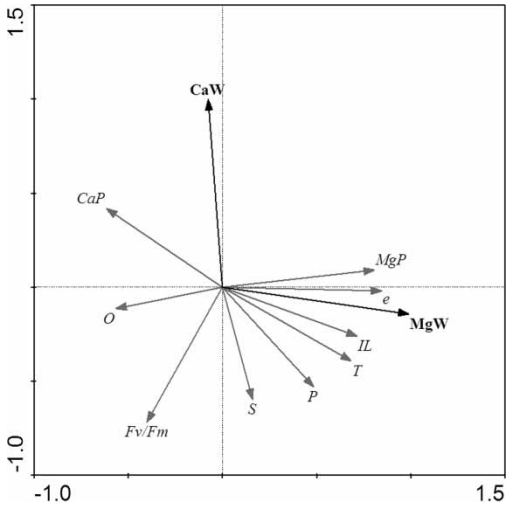

Figure 2. Redundancy analysis biplot diagram for experiment 1. Explanatory variables: Ca and Mg concentrations of water in (CaW, MgW). Response variables: Shoot elongation per week (e), Ca and Mg levels in plants (CaP, MgP). Internodal length (IL). Primary, secondary and tertiary branchlet lengths (P, S and T). Number of sexual propagules per plant (O) and maximum quantum efficiency of PSII photochemistry (F_v/F_m).

Table 3. Conditional effects of Ca and Mg concentrations in water (CaW and MgW) in order of their inclusion in the model.

Variable	Lamda-A	*p*	*F*
MgW	0.54	0.02*	11.59
CaW	0.02	0.62	0.53

Note: *Significant at $p < 0.05$.

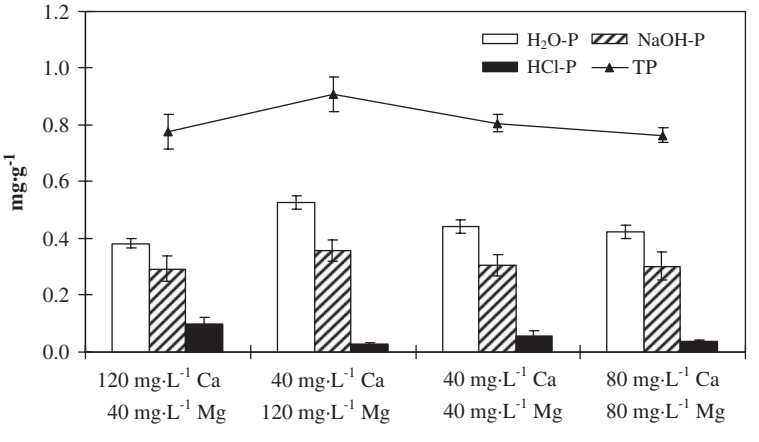

Figure 3. Total phosphorous (TP) and phosphorous speciation for Ca- and Mg-treated units after six months (experiment 2). H_2O-P, water soluble P; NaOH-P, nonreactive organic P; HCl-P, carbonate-bound P.

3.6. *Phosphorous speciation of* N. pseudoflabellata *and carbonate-bound Ca and Mg*

Figure 3 shows the P-speciation of *N. pseudoflabellata* at different combinations of Ca and Mg, measured after six months (i.e. experiment 2). With the increase in Mg, HCl-P seemed to be reduced. However, with the increase in Mg, total phosphorous showed relatively high values.

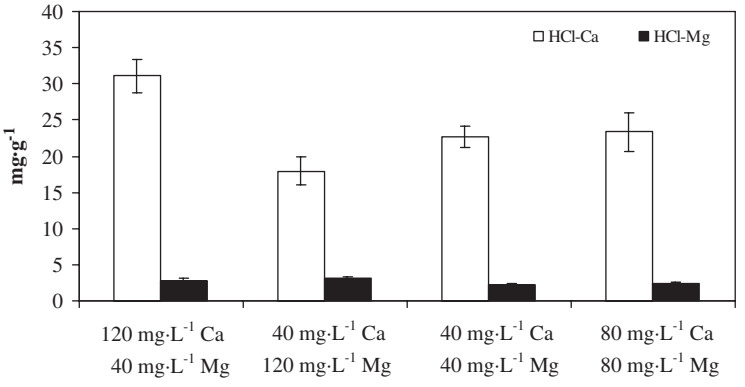

Figure 4. Ca and Mg levels in the extraction of carbonate-bound P (HCl-P) (experiment 2).

For example, the unit with 40 mg · L^{-1} Ca and 120 mg · L^{-1} Mg showed 0.91 mg · g^{-1} P, of which 0.52 mg · g^{-1} is H_2O-P. The high total phosphorous value can be attributed to the intensified growth as a result of Mg (as explained by experiment 1). However, this treatment gave the lowest HCl-P (0.02 mg · g^{-1} P). The unit with 120 mg · L^{-1} Ca and 40 mg · L^{-1} Mg showed the highest HCl-P (0.10 mg · g^{-1} P).

Figure 4 illustrates Ca and Mg levels in the extraction of HCl-P from plants harvested after six months (experiment 2). This will indicate the level of externally precipitated Ca and Mg. The lowest Ca level in HCl-P was observed in the unit with 40 mg · L^{-1} Ca and 120 mg · L^{-1} Mg. The same Ca concentration with a lower Mg concentration (40 mg · L^{-1} Ca and 40 mg · L^{-1} Mg) resulted in significantly high (ANOVA, $p < 0.05$) Ca level in HCl-P.

4. Discussion

4.1. *Impact of Ca and Mg on growth and morphological acclimations*

According to Imahori [9], the amount of Ca in water, and the subsequent calcification, correlate with its assimilation by charophytes. The carbon dioxide (CO_2) contained in calcium hydrogen carbonate is utilised by the charophytes during assimilation [9,20]. Wetzel and McGregor [33] stated that Ca concentrations of 20 mg · L^{-1} significantly reduced the photosynthesis rate of *Chara*. Similar observations have been reported by Vymazal [19]. Conflicting conclusions have been reported in the literature pertaining to the effect of Ca on growth in relation to concentration and duration. The results of an experiment with increasing Ca concentrations (Ca-treated units of experiment 1 conducted for 105 days) showed that the temporal variation in shoot elongation reduced over time; that is, the higher the Ca concentration, the earlier the phase of exponential growth (results not shown).

Magnesium is a constituent of chlorophyll, and thus is considered to be an absolute requirement for pigmented algae [19], deficiency results in the interruption of cell multiplication and many metabolic disturbances. In this study, Mg was observed to aid growth in terms of shoot elongation, and aid in the development of primary, secondary and tertiary branchlets. It should be noted that shorter internodes imply a short life-cycle for shoots [28].

4.2. *Stress physiology of plants*

Considering the physical measurements of the bioassay, the conclusion can be made that plants grown in Ca-treated units show a relatively retarded growth compared with plants grown in

Mg-treated units. The chlorophyll fluorescence results also suggest this. Although the use of chlorophyll fluorescence has a short history [34], it is gaining prominence as an important and reliable technique in plant physiology and has become ubiquitous [35,36]. Many of the associated fluorescence parameters can be used to assess the condition of plants. Maximum quantum efficiency of PSII photochemistry (F_v/F_m) is one such parameter. In Mg-treated units, F_v/F_m did not show proper correlation with Mg concentrations, but the presence of Mg $\geq 40\,\mathrm{mg \cdot L^{-1}}$ gave F_v/F_m values >0.8. Also, plants from Mg-treated units ($\geq 40\,\mathrm{mg \cdot L^{-1}}$ Mg) were greener. This is probably due to an increase in the chlorophyll content as a result of Mg availability [19]. A high F_v/F_m value suggests that the plant has a high chlorophyll content [37]. Furthermore, stress-free plants give F_v/F_m values >0.8 [34] and some reports indicate this threshold to be 0.76 [35]. Thus, it is fair to say that none of the treatments caused stress to the plants, however, the negative correlation between Ca concentrations and F_v/F_m values for Ca-treated units suggests that extremely high Ca concentrations may result in retarded growth in the long-term.

4.3. *Interrelationship of Ca and Mg accumulation in plants*

Examining the results of experiment 1 (Figure 2), it is apparent that Mg interacts with the processes of Ca accumulation, but not vice versa. In experiment 1, the Ca measured in plants includes the Ca in calcite. Thus, it is worth determining whether Mg acts on the external precipitation of $CaCO_3$ or on the internal absorption of Ca. It should be noted that intracellular Ca is submicromolar, whereas the concentration of the closely related divalent cation Mg is milimolar [38]. Despite a concentration difference that would favour Mg, cellular processes often display enormous selectivity for Ca [38]. Furthermore, Mg showed a strong positive correlation with many growth-related parameters, such as elongation per week (e) and internodal length (Figure 2). Thus, it is conspicuous that Mg is not affecting the Ca absorbing processes at a cellular level. Therefore, the negative correlation between Mg in water and Ca in plants (CaP) may be due to an interaction with the processes of $CaCO_3$ formation. Considering the Ca concentration in the HCl-P faction, we observed that it reduced with a relative and/or absolute increase in the Mg concentration in the water. This observation clearly demonstrates that Mg is interacting with the calcification process.

There are several hypotheses proposed to explain the link between calcification and cellular function [19]. Furthermore, $CaCO_3$ deposition is an inorganic precipitation caused by a high pH as a result of bicarbonate assimilation [39]. Bicarbonate assimilation requires an equal input of photons, thus plants rely on diffusion to supply photon equivalents. This bathes them in an alkaline, CO_2 depleted micro-environment [15]. Therefore, as a means of overcoming this problem, Charophytes cycle protons through their cells, creating acidic and alkaline zones [15]. $CaCO_3$ deposition occurs in these alkaline regions. McConnaughey [15] and Vymazal [19] showed that heavily calcified plants exhibit high rates of photosynthesis due to a lower amount of CO_2 leakage from cells to alkaline zones, because $CaCO_3$ reduces the permeability of the alkaline surface. Thus, calcification is partly due to algal photosynthesis [40]. Algal calcification can be inhibited or reduced by substances that interfere with algal metabolism, and also by poisoning of the crystal formation [40]. However, considering the Mg-aided growth of *N. pseudoflabellata*, the concept of inhibition of calcification by interfering algal metabolism is less important.

The influence of Mg on $CaCO_3$ formation has been studied extensively in chemical and processes engineering [41] and marine chemistry [42]. The impact of Mg interference on calcite formation in *N. pseudoflabellata* can be explained by the consumption of carbonate ions by Mg. This effectively reduces the free carbonate ions that are needed by Ca to precipitate as $CaCO_3$ [43]. Another explanation is the incorporation of Mg into the lattice, preventing further growth of $CaCO_3$ [41]. Chen et al. [41] stated that the incorporation of Mg ions in $CaCO_3$ crystal increased

the solubility of the $CaCO_3$. Compton and Brown [44] have stated that Mg will adsorb at lattice sites and subsequently compete for carbonates.

4.4. *Implications for P nutrient dynamics*

Rhizoid-bearing charophytes are known to acquire P and also other nutrients primarily from the water column [45]. By contrast, vascular plants acquire P mainly from sediment via their roots and this results in high P content in plant biomass [24]. This is the main reason for the high P values observed in vascular plant tissues relative to charophytes [24]. Thus, vascular plants can result in a reduction in nutrients in the water column. However, vascular submerged plants, upon senescence, release the accumulated P into the water column once more, making net P accumulation (in the long-term) zero. According to Shilla et al. [21] and Siong et al. [24] a high fraction of P in submerged vascular plants (such as *Najas marina*) is in a water-soluble form. However, charophytes can retain significantly more P in a nonwater-soluble form than can vascular plants [24]. According the results of this research, *N. pseudoflabellata* was able to contain ∼3–13% of P in a carbonate-bound form (HCl-P).

Decalcification, followed by co-precipitation of phosphate with $CaCO_3$, is an important process in the reduction of the bio-available P in the water column [26]. Carbonate-bound P in charophytes has been discussed by Kufel and Kufel [46], who examined sediment of a lake that had been dominated by charophytes. Kiyosawa [47] stated that calcified regions of charophytes included calcium hydrogen phosphate apart from $CaCO_3$. In the results of the current research, increases in Mg significantly reduced HCl-P, while maintaining a high percentage of P in H_2O-P. Thus, Mg is a constituent that seems to inhibit calcite growth and affect the P nutrient sink ability of charophytes.

5. Conclusion

Magnesium was seen to aid the growth of *N. pseudoflabellata*; however, the concentration range (40–120 $mg \cdot L^{-1}$ Mg) did not show significant differences in terms of shoot elongation or internodal length. With increasing Ca, the plants show greater elongation; however, internodal lengths were observed to be shortening. Thus, high Ca in water seemed to be unsuitable for plants in the long-term. Furthermore, depending on the availability of Ca or Mg, the morphological appearance differed significantly, indicating significant levels of ecoplasticity.

Magnesium was seen to inhibit calcite formation in plants. Subsequent speciation for P showed that the plants grown at the highest concentration of Mg contained the lowest HCl-P. However, they also contained the highest level of plant total phosphorous. This suggests that upon senescence and decomposition, a large fraction of P would be supplied to the water column. In this way, *N. pseudoflabellata* is ultimately behaving like a typical vascular plant. Therefore, it can be concluded Mg plays a vital role in charophyte habitats, influencing their morphological acclimations as well as the dynamics in nutrient cycling.

Acknowledgements

The authors would like to thank Prof. Takeshi Fujino and Dr Kian Siong for their support. This research was financially supported by a Research Grant-in-Aid from the Ministry of Education, Culture, Sports, Science and Technology, Japan.

References

[1] H. Coops, *Ecology of charophytes: an introduction*, Aquat. Bot. 72 (2002), pp. 205–208.
[2] Charophytes©. Available at: http://www.charophytes.com/cms/ (accessed 15 January 2009).

[3] J. John, *Phycoremediation: algae as tools for remediation of mine-void wetlands*, in R.S. Ambasht and N.K. Ambasht, eds., *Modern Trends in Applied Aquatic Ecology*, Kluwer Academic/Plenum Publishers, New York, 2003, pp. 133–147.
[4] P.I.A. Gomes and T. Asaeda, *Phycoremediation of chromium (VI) by* Nitella *and impact of calcium encrustation*, J. Hazard. Mater. 166 (2009), pp. 1332–1338.
[5] P. Guha, *Exploring ecological control of* Chara, Crop Protect. 14 (1995), pp. 527–528.
[6] M.T. Casanova and M.A. Brock, *Can oospore germination patterns explain charophyte distribution in permanent and temporary wetlands?* Aquat. Bot. 54 (1996), pp. 297–312.
[7] S.A. Crawford, *Chemical, physical and biological changes associated with* Chara *succession in farm ponds*, Hydrobiologia 55 (1977), pp. 209–217.
[8] C. Van den Hoek, D.G. Mann, and H.M. Jahns, *Algae: An Introduction to Phycology*, Cambridge University Press, Cambridge, 1996.
[9] K. Imahori, *Ecology, Phytogeography and Taxonomy of the Japanese Charophyta*, Kanagawa University, Japan, 1954.
[10] R.D. Wood, *Monograph of the Characeae. Volume 1*, in RD Wood and K Imahori, *A Revision of the Characeace*, Verlag von J. Cramer, Weinheim, 1965.
[11] M.T. Casanova, M.D. de Winton, K.G. Karol, and J.S. Clayton, Nitella hookeri *A. Braun (Characeae, Charophyceae) in New Zealand and Australia: implications for endemism, speciation and biogeography*, Charophytes 1(2007), pp. 2–18.
[12] N.C. Bueno and C.E. deM. Bicudo, *Temporal variation of* Nitella furcata *subsp*. mucronata *var.* mucronata *f*. oligospira *(Charophyceae) in the Ninféias pond, São Paulo State, southeast Brazil*, Acta. Bot. Bras. 20 (2006), pp. 1–11.
[13] H.G. Heumann, *Effects of heavy metals on growth and ultrastructure of* Chara vulgaris, Protoplasma 136 (1987), pp. 37–48.
[14] M. Okazaki and M. Tokita, *Calcification of* Chara braunii *(Charophyta) caused by alkaline band formation coupled with photosynthesis*, Jpn. J. Phycol. 36 (1988), pp. 193–201.
[15] T. McConnaughey, *Calcification in* Chara corallina: CO_2 *hydroxylation generates protons for bicarbonate assimilation*, Limnol. Oceanogr. 36 (1991), pp. 619–628.
[16] R.G. Wetzel, *Marl encrustation on hydrophytes in several Michigan lakes*, Oikos 11 (1960), pp. 223–236.
[17] K. Siong and T. Asaeda, *Does calcite encrustation in* Chara *provide a phosphorus nutrient sink?* J. Environ. Qual. 35 (2006), pp. 490–494.
[18] D. Shilla and J. Dativa, *Biomass dynamics of charophyte-dominated submerged macrophyte communities in Myall Lake, NSW, Australia*, Chem. Ecol. 24 (2008), pp. 367–377.
[19] J. Vymazal, *Algae and Element Cycling in Wetlands*, Lewis, Chelsea, MI, 1995.
[20] M.S. Van den Berg, H. Coops, J. Simons, and J. Pilon, *A comparative study of the use of inorganic carbon resources by* Chara aspera *and* Potamogeton pectinatus, Aquat. Bot. 72 (2002), pp. 219–233.
[21] D. Shilla, T. Asaeda, T. Fujino, and B. Sanderson, *Decomposition of dominant submerged macrophytes: implications for nutrient release in Myall Lake, NSW, Australia*, Wetl. Ecol. Manag. 14 (2006), pp. 427–433.
[22] A. Garcia, *Charophyta: their use in paleolimnology*, J. Paleolimnol. 10 (1994), pp. 43–52.
[23] M.A. Rodrigo, C. Rojo, M. Alvarez-Cobelas, and S. Cirujano, Chara hispida *beds as a sink of nitrogen: evidence from growth, nitrogen uptake and decomposition*, Aquat. Bot. 87 (2007), pp. 7–14.
[24] K. Siong, T. Asaeda, T. Fujino, and A. Redden, *Difference characteristics of phosphorous in* Chara *and two submerged angiosperm species: implications for phosphorous nutrient cycling in an aquatic ecosystem*, Wetl. Ecol. Manag. 14 (2006), pp. 505–510.
[25] M.A. Rodrigo and J.L. Alonso-Guillén, In situ *nitrate uptake rates in two* Chara *species*, Charophytes 1 (2008), pp. 49–54.
[26] A. Otsuki and R.G. Wetzel, *Coprecipitation of phosphate with carbonates in a marl lake*, Limnol. Oceanogr. 17 (1972), pp. 763–767.
[27] P. Anadón, R. Utrilla, A. Vázquez, *Mineralogy and Sr–Mg geochemistry of charophyte carbonates: a new tool for paleolimnological research*, Earth Planet. Sci. Lett. 197 (2002), pp. 205–214.
[28] T. Asaeda, L. Rajapakse, and B. Sanderson, *Morphological and reproductive acclimations to growth of two charophyte species in shallow and deep water*, Aquat. Bot. 86 (2007), pp. 393–401.
[29] I. Blindow, J. Dietrich, N. Mollmann, and H. Schubert, *Growth, photosynthesis and fertility of* Chara aspera *under different light and salinity conditions*, Aquat. Bot. 76(2003), pp. 213–234.
[30] American Public Health Association/American Water Works Association/Water Environment Federation, *Standard Methods for the Examination of Water and Wastewater*, 20th ed., APHA/AWWA/WEF, Washington, DC, 1998.
[31] J. Murphy and J. Riley, *A modified single solution method for the determination of phosphate in natural waters*, Anal. Chim. Acta. 27 (1962), pp. 31–36.
[32] C.J.F. Ter Braak and P. Smilauer, *CANOCO Reference Manual and CanoDraw for Windows User's Guide: Software for Canonical Community Ordination (Version 4.5)*, Microcomputer Power, Ithaca, NY, 2002.
[33] R.G. Wetzel and D.L. McGregor, *Axenic cultures and nutritional studies of aquatic macrophytes*, Am. Midl. Nat. 80 (1968), pp. 52–64.
[34] G.H. Mohammed, P. Zarco-Tejada, and J.R. Miller, *Applications of chlorophyll fluorescence in forestry and eco-physiology*, in J.R. DeEll and P.M.A. Toivonen, eds., *Practical Applications of Chlorophyll Fluorescence in Plant Biology*, Kluwer Academic, Boston, MA, 2003, pp. 79–124.
[35] K. Maxwell and G.N. Johnson, *Chlorophyll fluorescence – a practical guide*, J. Exp. Bot. 51 (2000), pp. 659–668.

[36] F.L. Figueroa, N. Korbee, P. Carrillo, J.M. Medina-Sánchez, M. Mata, J. Bonomi, and P.M. Sánchez-Castillo, *The effects of UV radiation on photosynthesis estimated as chlorophyll fluorescence in* Zygnemopsis decussata *(Chlorophyta) growing in a high mountain lake (Sierra Nevada, Southern Spain)*, J. Limnol. 68 (2009), pp. 206–216.
[37] J.-L. Mouget and G. Tremblin, *Suitability of the fluorescence monitoring system (FMS, Hansatech) for measurement of photosynthetic characteristics in algae*, Aquat. Bot. 74 (2002), pp. 219–231.
[38] P.K. Hepler and R.O. Wayne, *Calcium and plant development*, Annu. Rev. Plant Physiol. 36 (1985), pp. 397–439.
[39] M.A. Borowitzka, A.W.D. Larkum, and C.E. Nockolds, *A scanning electron microscope study of the structure and organization of the calcium carbonate deposits of algae*, Phycologia 13 (1974), pp. 195–203.
[40] C.R. Heath, B.C.S. Leadbeater, and M.E. Callow, *Effect of inhibitors on calcium carbonate deposition mediated by freshwater algae*, J. Appl. Phycol. 7 (1995), pp. 367–380.
[41] T. Chen, A. Neville, and M. Yuan, *Influence of Mg^{2+} on $CaCO_3$ formation – bulk precipitation and surface deposition*, Chem. Eng. Sci. 61 (2006), pp. 5318–5327.
[42] A.I. Rushdi, R.M. Pytkowicz, E. Suess, and C.T. Chen, *The effects of magnesium-to-calcium ratios in artificial seawater, at different ionic products, upon the induction time, and the mineralogy of calcium carbonate: a laboratory study*, Int. J. Earth Sci. 81 (1992), pp. 571–578.
[43] J.W. Morse, Dissolution *kinetics of calcium carbonate in seawater; V, Effects of natural inhibitors and position of the chemical lysocline*, Am. J. Sci. 274 (1974), pp. 638–647.
[44] R.G. Compton and C.A. Brown, *The inhibition of calcite dissolution/precipitation*, J. Colloid Interface Sci. 137 (1994), pp. 33–34.
[45] I. Kufel and L. Kufel, Chara *beds acting as nutrient sinks in shallow lakes – a review*, Aquat. Bot. 72 (2002), pp. 249–260.
[46] I. Kufel and L. Kufel, *Eutrophication process in a shallow, macrophytes-dominated lake: nutrient loading to and flow through Lake £uknajno (Poland)*, Hydrobiologia 342–343 (1997), pp. 387–394.
[47] K. Kiyosawa, *Ca^{2+} and phosphate releases from calcified* Chara *cell walls in concentrated KCl solution*, J. Exp. Bot. 52 (2001), pp. 223–229.